Photochemical & Photobiological Sciences

ROYAL SOCIETY OF CHEMISTRY

PAPER

View Article Online
View Journal

Cite this: DOI: 10.1039/c9pp00373h

Intramolecular interaction of synthetic chlorophyll heterodyads with different π-skeletons†

Hitoshi Tamiaki, * Kazuhiro Fukai and Soichi Nakamura

Received 6th September 2019,
Accepted 13th January 2020

DOI: 10.1039/c9pp00373h

rsc.li/pps

Two heterodyads were prepared from the chemical modification of naturally occurring (bacterio)chlorophyll-*a* and composed of a chlorin π-skeleton linked to a porphyrin or bacteriochlorin π-system. Zinc methyl pyropheophorbide-*a*, one of the chlorophyll-*a* derivatives, was covalently linked with its 17,18-didehydrogenated species (zinc methyl pyroprotopheophorbide-*a*) or its *trans*-7,8-dihydrogenated analog (zinc methyl pyrobacteriopheophorbide-*a* as one of the bacteriochlorophyll-*a* derivatives) through ethylene glycol diester at their 17-propionate residues. In benzene, the central zinc atoms of the synthetic conjugates were coordinated by two methanol molecules which were hydrogen-bonded with the 13-keto-carbonyl groups in a dyad molecule. The methanol locked, *y*-axis aligned, and slipped cofacial conformers showed two apparent Qy bands at longer wavelengths than those of the composite zinc complex monomers. The red-shifted Qy bands are ascribable to the exciton coupling of the two different π-systems in the folded heterodyad conformers. The synthetic heterodyads could be models of chlorophyll-*a*/*c* dimers in the light-harvesting antennas of chromophytes including fucoxanthin–chlorophyll proteins in diatoms and also chlorophyll-*a* species interacting with bacteriochlorophyll-*a* or *g* species in the charge-separating reaction centers of green sulfur bacteria or heliobacteria, respectively.

Introduction

Naturally occurring (bacterio)chlorophylls [(B)Chls] are categorized into three types of porphyrinoids: (i) Chl-*c* bearing a fully π-conjugated cyclic tetrapyrrole (porphyrin skeleton), (ii) Chls-*a*, *b*, *d*, and *f* as well as BChls-*c*, *d*, *e*, and *f* possessing a *trans*-17,18-dihydroporphyrin π-system (chlorin skeleton), and (iii) BChls-*a*, *b*, and *g* having a bacteriochlorin π-skeleton with two single bonds at the β-positions of the opposite pyrrole rings (Fig. 1).[1] In photosynthetic apparatuses, the same (B)Chl molecules often interact with each other to give specific supramolecules. In almost all oxygen-evolving photosystem (PS) 2, two or four Chl-*a* molecules are closely situated to form P680 with a red-most (Qy) absorption maximum at 680 nm.[2] Two BChl-*a* molecules are excitonically coupled in the charge-separating reaction center (RC) of most purple bacteria, yielding a special pair with a Qy maximum at around 870 nm.[3]

In contrast, it has been observed in some phototrophs that (B)Chl molecules with different π-skeletons can come into close contact with each other. Chromophytes, including heterokontophytes, haptophytes, cryptophytes, and dinophytes, contain Chls-*a* and *c* pigments.[4] In their light-harvesting antenna systems, the Chl-*c* molecules are always near the Chl-*a* molecules, causing some interactions of the different π-systems. Recently, a fucoxanthin and Chl-*a*/*c* binding protein (FCP), one of the light-harvesting antenna systems in a diatom belonging to Heterokontophyta, was revealed at an atomic level by crystallographic analysis.[5] In the FCP crystal, Chl-c_1 (8-ethyl analog) 408 partially overlaps with Chl-*a* 401 at a closest π–π distance of 3.9 Å and an Mg–Mg distance of 10.6 Å, while Chl-c_2 (8-vinyl analog) 403 is near Chl-*a* 406 with 3.4 Å π–π and 9.0 Å Mg–Mg distances (Fig. S1†). The dimers are formed due to the interaction between the C/E-rings of the composite Chl molecules.

PS1-type RCs of anoxygenic photosynthetic bacteria, heliobacteria, green sulfur bacteria (GSB), and chloroacidobacteria contain both bacteriochlorin and chlorin chromophores.[6] The RC proteins of heliobacteria were successfully determined at a 2.2 Å resolution.[7] In heliobacterial RCs, a BChl-*g* molecule is located near the Chl-*a* species, farnesylated 8^1-hydroxy-Chl-*a*, with an Mg–Mg distance of 9.1 Å, where the former A/B-rings are directed toward the latter A/B-rings (Fig. S2†). Although crystallographic data for GSB–RC complexes are not yet available, a BChl-*a* molecule or its 13^2-epimer (BChl-*a*′) must be situated near the Chl-*a* species, 2,6-phytadienylated Chl-*a*, in the RC system.[8] Moreover, the main light-harvesting antenna systems called chlorosomes of GSB and filamentous anoxygenic phototrophs contain bacteriochlorin BChl-*a* and chlorin BChls-*c*/*d*/*e*/*f* pigments.[9] There are self-aggregates of

Graduate School of Life Sciences, Ritsumeikan University, Kusatsu, Shiga 525-8577, Japan. E-mail: tamiaki@fc.ritsumei.ac.jp

†Electronic supplementary information (ESI) available. See DOI: 10.1039/c9pp00373h

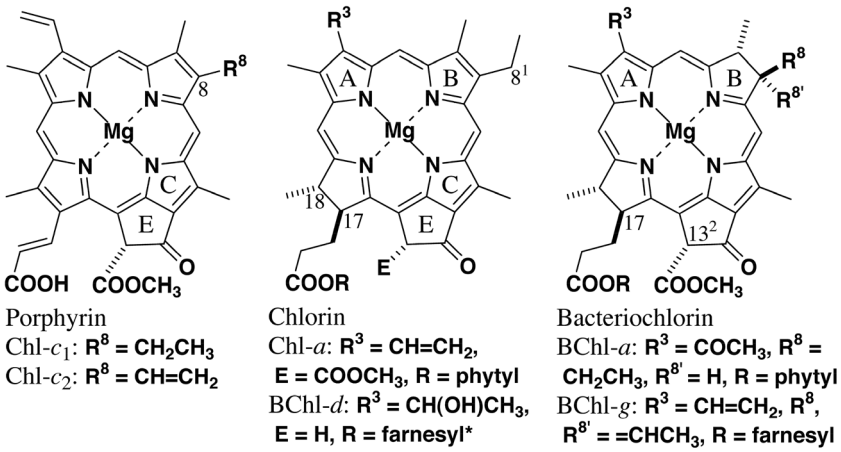

Fig. 1 Representative naturally occurring (B)Chls with porphyrin (left), chlorin (center), and bacteriochlorin π-system (right). *The molecular structure is one of several BChl-*d* homologs.

BChl-*c*, *d*, *e*, or *f* molecules in the core part of the chlorosomes that can transfer their excitation energy to BChl-*a* molecules in the periphery (baseplate proteins).[10]

As models of the aforementioned (B)Chl dimers, covalently linked dyads of (B)Chl derivatives possessing the same cyclic tetrapyrrole π-system were prepared, and their optical properties were investigated in a solution.[11,12] In particular, synthetic (B)Chl-*a* homodyads linked with an ethylene glycol diester at the 17-propionate were useful for the construction of their folded conformers by specific bondings with two methanol molecules (see Fig. 2), which were confirmed by ^{1}H NMR analysis.[13–16] In the resulting supramolecules, two π-systems excitonically interacted to give red-shifted Qy bands, as in the dimers of natural RCs. Here, we report the first preparation of methanol-locked conformers of Zn-(B)Chl-*a* derivative heterodyads bearing different π-skeletons, namely chlorin–porphyrin and bacteriochlorin–chlorin. The electronic absorption spectra of these heterodyads in benzene showed redshifted Qy bands. Such folded conformers of the heterodyads are valuable for understanding the electronic interaction of (B)Chls bearing different π-systems observed in the natural photosynthetic apparatus (*vide supra*).

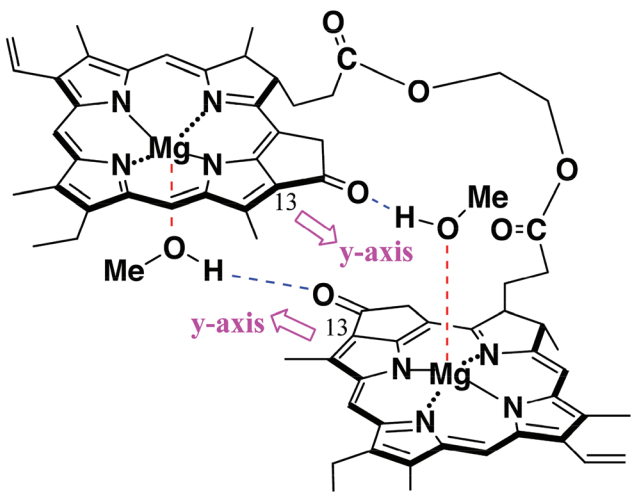

Fig. 2 Folded conformer of a synthetic Chl-*a* derivative homodyad assisted by methanol.

Materials and methods

General

Electronic absorption and circular dichroism (CD) spectra were measured with a Hitachi U-3500 spectrometer (Tokyo, Japan) and a JASCO J-720W spectrometer (Hachioji, Japan), respectively. ^{1}H NMR spectra were measured at room temperature with a JEOL ECA-600 (600 MHz) spectrometer (Akishima, Japan); chemical shifts (δ) are expressed in parts per million relative to residual chloroform (δ = 7.26 ppm) as an internal reference. Proton peaks were assigned using ^{1}H–^{1}H two-dimensional NMR techniques. Time-of-flight mass spectra (TOF-MS) were obtained using direct laser desorption/ionization (LDI) using a Shimadzu AXIMA-CFR*plus* spectrometer (Kyoto, Japan). Flash column chromatography (FCC) was performed with silica gel (Wakogel C-300, FUJIFILM Wako Pure Chem., Osaka, Japan). HPLC data were collected using a Shimadzu LC-10ADvp pump and SPD-M10Avp photodiode-array detector equipped with an octadecylated column (Cosmosil 5C_{18}AR-II, Nacalai Tesque, Kyoto, Japan).

Pyropheophorbide-*a*,[16,17] pyrobacteriopheophorbide-*a*,[16,18] 2-hydroxyethyl pyropheophorbide-*a*,[15,17] methyl pyroprotopheophorbide-*a* (**H_2P**),[19] zinc methyl pyropheophorbide-*a* (**ZnC**),[19] and zinc methyl pyrobacteriopheophorbide-*a* (**ZnB**)[18,20] were prepared according to the reported procedures. All the reaction reagents and solvents except those mentioned below were obtained from commercial suppliers and utilized as supplied. Dry dichloromethane for esterification was freshly distilled over calcium hydride before use. Benzene, methanol, and pyridine for electronic absorption and CD spectral

measurements were purchased from Nacalai Tesque as reagents prepared specially for spectroscopy and used without further purification. All the reactions were performed under a nitrogen atmosphere in the dark.

Synthesis of 2-hydroxyethyl pyroprotopheophorbide-*a*

Concentrated sulfuric acid (2.0 ml) was added to an ice-chilled mixture of ethylene glycol (20.0 ml) and methyl ester **H_2P** (26.6 mg, 48.7 μmol). After stirring for 5 h at room temperature (rt), the mixture was poured into ice water and extracted with chloroform. The organic layer was washed with an aqueous 4% sodium hydrogen carbonate solution and water and dried over sodium sulfate. After evaporation of the solvent, the residue was purified by FCC with dichloromethane and 2% methanol and recrystallized from dichloromethane and hexane to give the corresponding 2-hydroxyethyl ester (20.8 mg, 36.1 μmol, 74% yield): VIS (CH_2Cl_2) λ_{max} = 590 (relative intensity, 0.07), 568 (0.09), 524 (0.04), 420 nm (1.00); ^{1}H NMR ($CDCl_3$) δ = 9.87, 9.78, 9.55 (each 1H, s, 5-, 10-, 20-H), 8.16 (1H, dd, J = 18, 12 Hz, 3-CH), 6.29 (1H, d, J = 18 Hz, 3^1-CH *trans* to 3-C–H), 6.18 (1H, d, J = 12 Hz, 3^1-CH *cis* to 3-C–H), 5.39 (2H, s, 13^1-CH_2), 4.29 (2H, t, J = 5 Hz, 17^2-$COOCH_2$), 3.99 (2H, q, J = 8 Hz, 8-CH_2), 3.87 (2H, t, J = 8 Hz, 17-CH_2), 3.83 (2H, t, J = 5 Hz, 17^2-$COOCCH_2$), 3.73, 3.57, 3.56, 3.37 (each 3H, s, 2-, 7-, 12-, 18-CH_3), 2.89 (2H, t, J = 8 Hz, 17^1-CH_2), 1.83 (3H, t, J = 8 Hz, 8^1-CH_3), −3.24, −4.41 (each 1H, s, NH × 2); TOF-MS (LDI) m/z 576.5 (M^-), calcd for $C_{35}H_{36}N_4O_4$: 576.3.

Synthesis of the ethylene pyropheophorbide-*a*–pyroprotopheophorbide-*a* dyad (H_2C–H_2P)

1-Ethyl-3-(3-dimethyaminopropyl)carbodiimide hydrochloride (EDC·HCl, 30.4 mg, 159 μmol) and 4-(dimethylamino)pyridine (DMAP, 40.4 mg, 331 μmol) were added to an ice-chilled solution of acidic pyropheophorbide-*a* (10.4 mg, 19.5 μmol) and the above-synthesized alcoholic 2-hydroxyethyl pyroprotopheophorbide-*a* (6.3 mg, 10.9 μmol) in dry dichloromethane (10 ml). After stirring for 18 h at rt, the mixture was poured into an aqueous 2% hydrogen chloride solution and extracted with dichloromethane. The organic layer was worked up similarly as in the synthesis of the above 2-hydroxyethyl ester to give the corresponding esterified dyad **H_2C–H_2P** (10.9 mg, 10.0 μmol, 91% yield): VIS (CH_2Cl_2) λ_{max} = 674 (relative intensity, 0.20), 603 (0.09), 571 (0.09), 542 (0.08), 514 (0.08), 415 (1.00), 403 nm (1.00); ^{1}H NMR ($CDCl_3$) δ (the prefix c/p indicates **H_2C**/**H_2P** moieties) = 10.40 (1H, s, p5-H), 10.20 (1H, s, p10-H), 9.75 (1H, s, p20-H), 8.78 (1H, s, c20-H), 8.58 (1H, dd, J = 18, 12 Hz, p3-CH), 8.46 (1H, s, c10-H), 7.59 (1H, s, c5-H), 7.27 (1H, dd, J = 17.5, 11.5 Hz, c3-CH), 6.53 (1H, d, J = 18 Hz, p3^1-CH *trans* to C3–H), 6.30 (1H, d, J = 12 Hz, p3^1-CH *cis* to C3–H), 5.87 (1H, d, J = 17.5 Hz, c3^1-CH *trans* to C3–H), 5.78 (1H, d, J = 11.5 Hz, c3^1-CH *cis* to C3–H), 5.61, 5.13 (each 1H, d, J = 18 Hz, p13^1-CH_2), 4.61 (1H, m, c18-H), 4.60, 4.29 (each 2H, t, J = 7 Hz, 17^2-$COOCH_2CH_2$), 4.30 (1H, br-d, c17-H), 4.17 (1H, d, J = 19 Hz, c13^1-CH *trans* to C17–H), 4.10 (2H, q, J = 8 Hz, p8-CH_2), 3.76 (1H, d, J = 19 Hz, c13^1-CH *cis* to C17–H), 3.75 (3H, s, p2-CH_3), 3.64 (3H, s, p12-CH_3), 3.61 (3H, s, p7-CH_3), 3.47–3.44, 3.35–3.32, 2.82–2.74, 2.62–2.53 (each 1H, m, p17-CH_2CH_2), 3.42 (3H, s, c12-CH_3), 3.32 (3H, s, c2-CH_3), 3.04–2.97, 2.75–2.69 (each 1H, m, c17^1-CH_2), 2.93 (3H, s, p18-CH_3), 2.90–2.82, 2.66–2.59 (each 1H, m, c17-CH_2), 2.47, 2.14 (each 1H, m, c8-CH_2), 1.89 (3H, t, J = 8 Hz, p8^1-CH_3), 1.74 (3H, d, J = 8 Hz, c18-CH_3), 1.47 (3H, s, c7-CH_3), 0.96 (3H, t, J = 8 Hz, c8^1-CH_3), −0.36, −2.50, −2.52, −4.45 (each 1H, s, NH × 4); TOF-MS (LDI) m/z 1094.1 (MH^+), calcd for $C_{68}H_{69}N_8O_6$: 1093.5.

Synthesis of the ethylene zinc pyropheophorbide-*a*–zinc pyroprotopheophorbide-*a* dyad (ZnC–ZnP)

Zinc acetate dihydrate (200 mg) in methanol (10 ml) was added to the above free base dyad **H_2C–H_2P** (10.9 mg, 10.0 μmol) in chloroform (20 ml). After stirring for 5 h at rt, the reaction mixture was worked up similarly as in the synthesis of the above dyad and purified with HPLC (retention time was 21.6 min, Cosmosil 5C_{18}-AR-II 10 ∅ × 250 mm, CH_3OH, 2.0 ml min^{-1}) to give the corresponding dizinc complex **ZnC–ZnP** quantitatively: VIS (C_6H_6-1% C_5H_5N) λ_{max} = 662 (relative intensity, 0.21), 620 (0.12), 572 (0.06), 437 nm (1.00); ^{1}H NMR ($CDCl_3$-1% C_5D_5N) δ (prefixed c/p indicate **ZnC**/**ZnP** moieties) = 9.93 (1H, s, p10-H), 9.83 (1H, s, p5-H), 9.61 (1H, s, p20-H), 9.26 (1H, s, c10-H), 8.89 (1H, s, c5-H), 8.27 (1H, s, c20-H), 8.25 (1H, dd, J = 18, 11 Hz, p3-CH), 7.79 (1H, dd, J = 18, 11 Hz, c3-CH), 6.34 (1H, d, J = 18 Hz, p3^1-CH *trans* to C3–H), 6.13 (1H, d, J = 11 Hz, p3^1-CH *cis* to C3–H), 6.04 (1H, d, J = 18 Hz, c3^1-CH *trans* to C3–H), 5.88 (1H, d, J = 11 Hz, c3^1-CH *cis* to C3–H), 5.55, 5.47 (each 1H, d, J = 19 Hz, p13^1-CH_2), 5.14 (1H, d, J = 19 Hz, c13^1-CH *trans* to C17–H), 4.99 (1H, d, J = 19 Hz, c13^1-CH *cis* to C17–H), 4.35 (1H, q, J = 8 Hz, c18-H), 4.27, 4.21 (each 2H, m, 17^2-$COOCH_2CH_2$), 4.09 (1H, br-d, c17-H), 3.95 (2H, q, J = 8 Hz, p8-CH_2), 3.83–3.80 (2H, m, p17-CH_2), 3.82 (3H, s, p12-CH_3), 3.62 (3H, s, p2-CH_3), 3.57 (3H, s, c12-CH_3), 3.47 (3H, s, p7-CH_3), 3.43, 3.37 (each 1H, dq, J = 15, 8 Hz, c8-CH_2), 3.28 (3H, s, p18-CH_3), 3.24 (3H, s, c2-CH_3), 2.90 (2H, dd, J = 7, 10 Hz, p17^1-CH_2), 2.87 (3H, s, c7-CH_3), 2.53–2.46, 2.22–2.16 (each 1H, m, c17-CH_2), 2.46–2.38, 2.00–1.96 (each 1H, m, c17^1-CH_2), 1.82 (3H, t, J = 8 Hz, p8^1-CH_3), 1.61 (3H, d, J = 8 Hz, c18-CH_3), 1.53 (3H, t, J = 8 Hz, c8^1-CH_3); TOF-MS (LDI) m/z 1220.9 (M^+), calcd for $C_{68}H_{64}N_8O_6Zn_2$: 1220.4.

Synthesis of the ethylene pyrobacteriopheophorbide-*a*–pyropheophorbide-*a* dyad (H_2B–H_2C)

Similar to the synthesis of chlorin–porphyrin dyad **H_2C–H_2P**, condensation of acidic pyrobacteriopheophorbide-*a* (3.8 mg, 6.9 μmol) with alcoholic 2-hydroxyethyl pyropheophorbide-*a* (4.7 mg, 8.1 μmol) using EDC·HCl (20.3 mg, 106 μmol) and DMAP (22.4 mg, 183 μmol) afforded the corresponding esterified dyad **H_2B–H_2C** (7.1 mg, 6.4 μmol, 93% yield): VIS (CH_2Cl_2) λ_{max} = 755 (relative intensity, 0.32), 668 (0.45), 612 (0.09), 536 (0.20), 414 (1.00), 393 (0.95), 363 nm (0.91); ^{1}H NMR ($CDCl_3$) δ (prefixed b/c indicate **H_2B**/**H_2C** moieties) = 9.44 (1H, s, c10-H), 9.32 (1H, s, c5-H), 8.97 (1H, s, b5-H), 8.51 (1H, s, b10-H), 8.43 (1H, s, c20-H), 8.30 (1H, s, b20-H), 7.94 (1H, dd, J = 18, 12 Hz, c3-CH), 6.23 (1H, d, J = 18 Hz, c3^1-CH *trans* to C3–H),

6.13 (1H, d, J = 12 Hz, c3^1-CH *cis* to C3–H), 5.20 (1H, d, J = 19 Hz, c13^1-CH *trans* to C17–H), 5.03 (1H, d, J = 19 Hz, c13^1-CH *cis* to C17–H), 4.98 (1H, d, J = 19 Hz, b13^1-CH *cis* to C17–H), 4.78 (1H, d, J = 19 Hz, b13^1-CH *trans* to C17–H), 4.43 (1H, br-q, c18-H), 4.25 (1H, br-q, b7-H), 4.22 (1H, br-d, c17-H), 4.17 (1H, br-q, b18-H), 4.12 (4H, br, 17^2-$COOCH_2CH_2$), 4.01 (1H, br-d, b8-H), 3.96 (1H, br-d, b17-H), 3.64 (2H, q, J = 8 Hz, c8-CH_2), 3.62 (3H, s, c12-CH_3), 3.41 (3H, s, b12-CH_3), 3.37 (3H, s, b2-CH_3), 3.34 (3H, s, c2-CH_3), 3.19 (3H, s, c7-CH_3), 3.10 (3H, s, b3^1-CH_3), 2.63–2.59, 2.56–2.51, 2.26–2.22 (1H + 1H + 2H, m, c17-CH_2CH_2), 2.47–2.42, 2.20–2.16 (each 1H, m, b17^1-CH_2), 2.47–2.42, 2.11–2.06 (each 1H, m, b17-CH_2), 2.33–2.29, 2.04–1.99 (2H, m, b8-CH_2), 1.79 (3H, d, J = 7 Hz, b7-CH_3), 1.73 (3H, d, J = 7 Hz, c18-CH_3), 1.66 (3H, t, J = 8 Hz, c8^1-CH_3), 1.58 (3H, d, J = 7 Hz, b18-CH_3), 1.07 (3H, t, J = 7 Hz, b8^1-CH_3), 0.41, 0.26, −1.13, −1.74 (each 1H, s, NH × 4); TOF-MS (LDI) m/z 1112.7 (M^-), calcd for $C_{68}H_{72}N_8O_7$: 1112.6.

Synthesis of the ethylene zinc pyrobacteriopheophorbide-*a*–zinc pyropheophorbide-*a* dyad (ZnB–ZnC)

Similar to the synthesis of the zinc chlorin–zinc porphyrin dyad **ZnC–ZnP**, the above free base dyad **H_2B–H_2C** (7.1 mg, 6.4 μmol) was zinc-metallated after refluxing for 18 h to give the corresponding dizinc complex **ZnB–ZnC** (retention time of HPLC = 17.9 min) quantitatively: VIS (C_6H_6-1% C_5H_5N) λ_{max} = 775 (relative intensity, 0.69), 660 (0.60), 579 (0.21), 433 (1.00), 405 (0.61), 365 nm (0.68); ^{1}H NMR ($CDCl_3$-1% C_5D_5N) δ (the prefix b/c indicates **ZnB**/**ZnC** moieties) = 9.52 (1H, s, c10-H), 9.25 (1H, s, c5-H), 8.79 (1H, s, b5-H), 8.37 (1H, s, b10-H), 8.31 (1H, s, c20-H), 8.19 (1H, s, b20-H), 8.00 (1H, dd, J = 18, 11 Hz, c3-CH), 6.16 (1H, d, J = 18 Hz, c3^1-CH *trans* to C3–H), 6.01 (1H, d, J = 11 Hz, c3^1-CH *cis* to C3–H), 5.15 (1H, d, J = 19 Hz, c13^1-CH *trans* to C17–H), 5.03 (1H, d, J = 19 Hz, c13^1-CH *cis* to C17–H), 4.97 (1H, d, J = 19 Hz, b13^1-CH *cis* to C17–H), 4.84 (1H, d, J = 19 Hz, b13^1-CH *trans* to C17–H), 4.35 (1H, q, J = 7 Hz, c18-H), 4.19 (1H, br-q, J = 7 Hz, b7-H), 4.15 (1H, br-q, J = 7 Hz, b18-H), 4.15 (1H, br-d, c17-H), 4.06, 4.05 (each 2H, br, 17^2-$COOCH_2CH_2$), 3.98 (2H, br-d, b8-, b17-H), 3.73 (2H, q, J = 8 Hz, c8-CH_2), 3.65 (3H, s, c12-CH_3), 3.42 (3H, s, b12-CH_3), 3.38 (3H, s, b2-CH_3), 3.31 (3H, s, c2-CH_3), 3.23 (3H, s, c7-CH_3), 3.06 (3H, s, b3^1-CH_3), 2.53–2.46, 2.27–2.18 (each 1H, m, c17-CH_2), 2.44–2.37, 2.15–2.09 (each 1H, m, b17-CH_2), 2.36–2.30, 2.00–1.94 (each 2H, m, c17^1-, b17^1-CH_2), 2.27–2.22, 2.03–1.96 (2H, m, b8-CH_2), 1.69 (3H, d, J = 7 Hz, b7-CH_3), 1.68 (3H, t, J = 8 Hz, c8^1-CH_3), 1.66 (3H, d, J = 7 Hz, c18-CH_3), 1.57 (3H, d, J = 7 Hz, b18-CH_3), 0.92 (3H, t, J = 8 Hz, b8^1-CH_3); TOF-MS (LDI) m/z 1239.9 (M^+), calcd for $C_{68}H_{68}N_8O_7Zn_2$: 1240.4.

Synthesis of zinc methyl pyroprotopheophorbide-*a* (ZnP)

Similar to the synthesis of the zinc chlorin–zinc porphyrin dyad **ZnC–ZnP**, free base porphyrin **H_2P** was zinc-metallated to give the corresponding zinc complex **ZnP** in a nearly quantitative yield: see the spectral data in ref. 21 and 22.

Results and discussion

Synthesis of heterodyads

Chl-*a* was obtained from commercially available spirulina powders and dry cells of cultured cyanobacterial species, and was chemically modified to methyl pyropheophorbide-*a* (**H_2C**) according to the reported procedures (Fig. 3).[23] The methyl

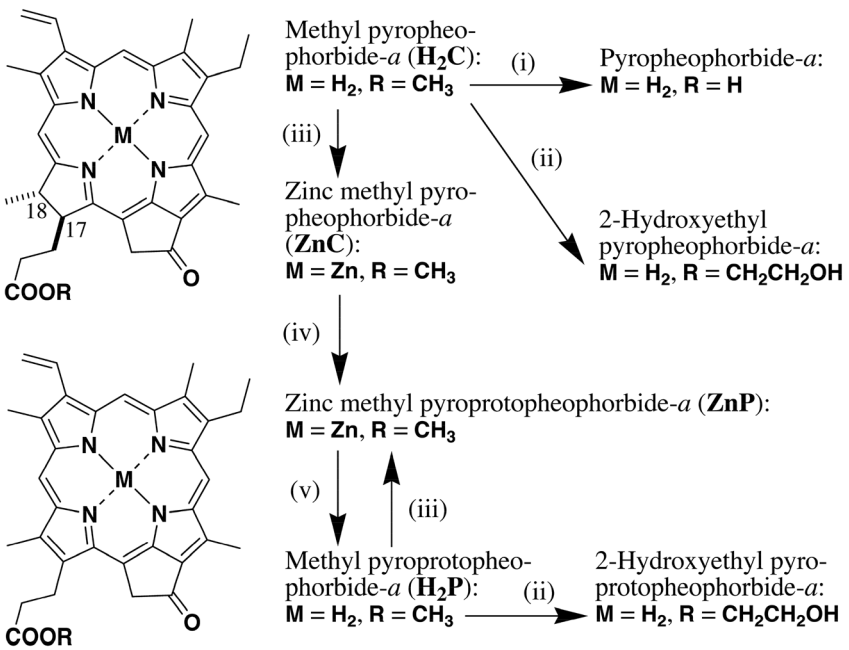

Fig. 3 Synthesis of (zinc) pyro(proto)pheophorbides-*a* by chemically modifying **H_2C** prepared from naturally occurring Chl-*a*: (i) conc. HCl/acetone, 0 °C to rt; (ii) $HOCH_2CH_2OH$, conc. H_2SO_4, 0 °C to rt; (iii) $Zn(OAc)_2{\cdot}2H_2O/CH_3OH–CHCl_3$, rt; (iv) DDQ/acetone, rt; (v) conc. HCl/CH_2Cl_2, rt.

ester of **H_2C** was quantitatively hydrolyzed by the action of hydrochloric acid to pyropheophorbide-*a* bearing a free 17-propionate residue [see step (i)],[16] and *trans*-esterified with ethylene glycol in the presence of sulfuric acid to the corresponding 2-hydroxyethyl ester in 91% yield [step (ii)].[15] Free base **H_2C** was zinc-metallated to **ZnC** in a nearly quantitative yield [step (iii)].[19] Chlorin **ZnC** was 17,18-dehydrogenated by 2,3-dichloro-5,6-dicyano-1,4-benzoquinone (DDQ) to afford fully π-conjugated **ZnP** [step (iv)], followed by demetallation to give pure **H_2P** after silica gel column chromatography in 77% overall yield [step (v)].[19] It is noted that the DDQ-dehydrogenation of **H_2C** afforded a complex mixture containing a small amount of **H_2P**, but **ZnC** was readily oxidized to **ZnP** by zinc-metallation due to its oxidation lability. The methyl ester of **H_2P** was transformed into the corresponding 2-hydroxyethyl ester in 74% yield by step (ii) and zinc complex **ZnP** in a nearly quantitative yield by step (iii). The purification of **ZnP** by conventional chromatography was relatively difficult in comparison with that of **H_2P**, so its pure sample was difficult to obtain only by the direct oxidation of **ZnC**.

Following the reported procedures,[24] methyl pyrobacteriopheophorbide-*a* (**H_2B**) was prepared by modifying BChl-*a* obtained from cultured purple bacterial cells (Fig. 4). The methyl ester of **H_2B** was hydrolyzed to its carboxylic acid, pyrobacteriopheophorbide-*a*, in 93% yield [step (i)].[18] At a high temperature, **H_2B** was zinc-metallated to **ZnB** in 66% yield [step (vi)].[18] The zinc metallation of bacteriochlorin as in **H_2B** to **ZnB** was requisite for refluxing in a 2 : 1 mixture of chloroform and methanol, whereas those of chlorin (**H_2C** → **ZnC**) and porphyrin (**H_2P** → **ZnP**) proceeded smoothly by stirring in the same solvent at rt [*vide supra*, step (iii)]. The difference in the chemical reactivity as in **H_2C**, **H_2P** > **H_2B** is consistent with the previous report.[25] During the above chemical modification in the dark under nitrogen, no oxidation was observed from its bacteriochlorin to the chlorin π-system through 7,8-dehydrogenation.

The esterification of acidic pyropheophorbide-*a* with alcoholic 2-hydroxyethyl pyroprotopheophorbide-*a* was achieved by the action of a water-soluble carbodiimide (EDC) as a condensation reagent with DMAP as a condensation accelerating reagent. This conventional coupling reaction (see Scheme S1†) gave the corresponding chlorin and porphyrin conjugate linked with ethylene glycol diester **H_2C–H_2P** in 91% yield [step (vii) of Fig. 5, upper]. The free bases were doubly zinc-metallated to afford **ZnC–ZnP** quantitatively [step (iii)]. Similarly, the zinc bacteriochlorin and zinc chlorin dyad **ZnB–ZnC** was obtained by the esterification of pyrobacteriopheophorbide-*a* with 2-hydroxyethyl pyropheophorbide-*a* (93%) and successively clean zinc metallation of the resulting dyad **H_2B–H_2C** as shown in the lower part of Fig. 5.

Electronic absorption spectra of the heterodyads

The synthetic conjugate **ZnC–ZnP** of zinc chlorin and zinc porphyrin covalently linked with an ethylene glycol diester was dissolved in benzene (*ca.* 5 μM), to which was added 1% (v/v) pyridine. The solution showed a sharp Soret band at 437 nm (the dotted line in Fig. 6, upper part). Additionally, two relatively small bands were observed at 662 and 620 nm. The former was assigned to the main Qy [= Qy(0,0)] maximum of the zinc chlorin moiety, and the latter was primarily ascribable to the Qy(0,0) peak of the zinc porphyrin part. In the solution, pyridine molecules coordinated to the central zinc atoms of the planar zinc chlorin and porphyrin moieties to form the pyramidal configurations. Therefore, the two 5-coordinated species hardly interacted in this dyad because their spectral features are consistent with those of monomeric species.

In contrast, the addition of 1% (v/v) methanol to the benzene solution of **ZnC–ZnP** afforded a broadened Soret band and red-shifted Qy bands (the solid line in Fig. 6, upper part). Methanol molecules coordinated to the zinc atoms similarly as pyridine molecules to give the axially coordinated species. The coordinating methanolic hydroxy groups additionally hydrogen-bonded with the keto-carbonyl groups at the 13-position to form a folded conformer (see Fig. 2). The double coordinations and hydrogen-bonds of two methanol molecules to a single **ZnC–ZnP** molecule produced a π–π interaction species. The slipped cofacial conformer along the molecular *y*-axis of the composite (bacterio)chlorins induced J-type stacking to shift the Qy maxima bathochromically. The excitonically coupled conformation was supported by

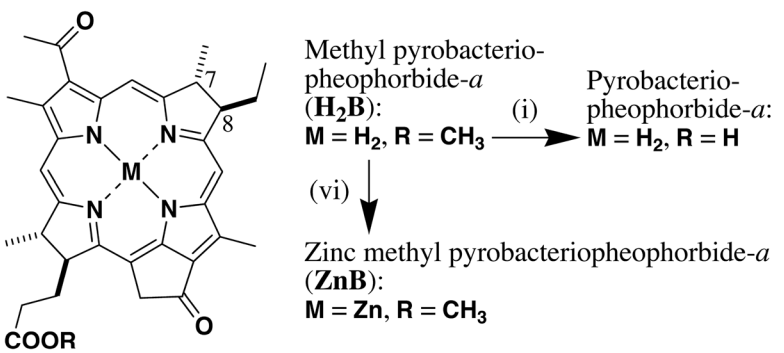

Fig. 4 Synthesis of (zinc) pyrobacteriopheophorbides-*a* by chemically modifying H_2B prepared from naturally occurring BChl-*a*: (i) conc. HCl/acetone, 0 °C to rt; (vi) $Zn(OAc)_2{\cdot}2H_2O/CH_3OH–CHCl_3$, reflux.

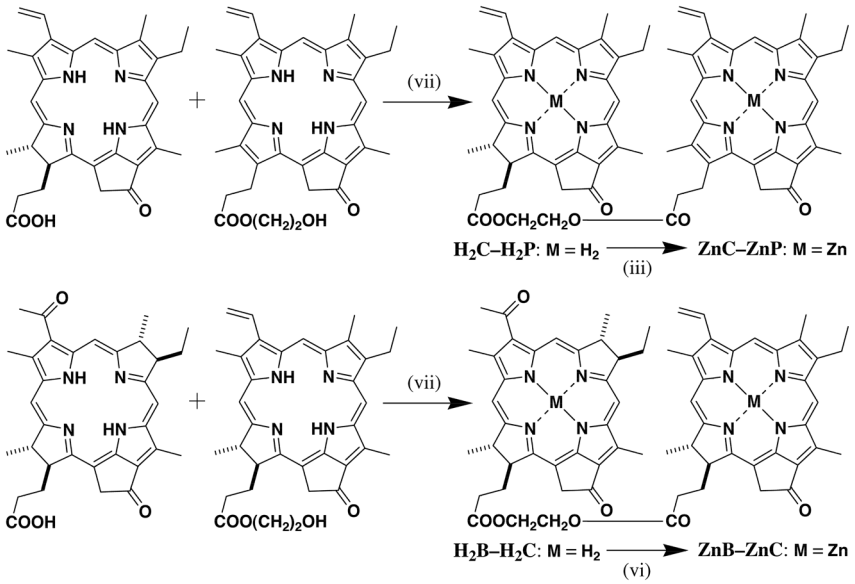

Fig. 5 Synthesis of chlorin–porphyrin and bacteriochlorin–chlorin heterodyads: (iii) $Zn(OAc)_2{\cdot}2H_2O/CH_3OH–CHCl_3$, rt; (vi) $Zn(OAc)_2{\cdot}2H_2O/CH_3OH–CHCl_3$, reflux; (vii) EDC·HCl, DMAP/CH_2Cl_2, 0 °C to rt.

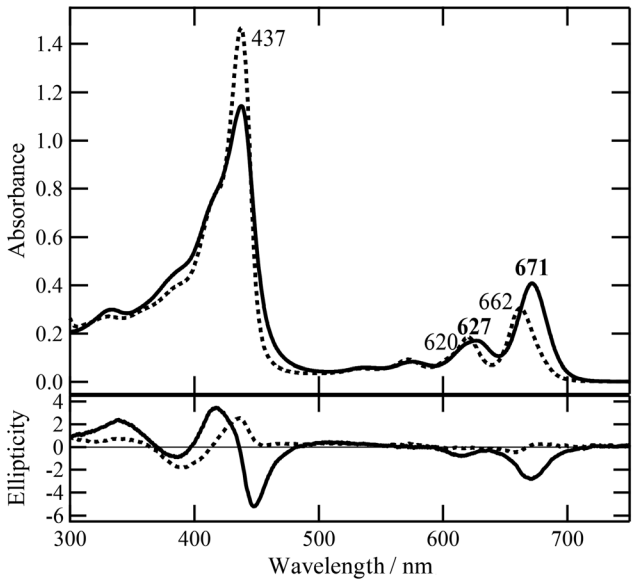

Fig. 6 Electronic absorption (upper) and CD spectra (lower) of **ZnC–ZnP** (5 μM) in benzene with 1% (v/v) methanol (solid lines) and pyridine (dotted lines).

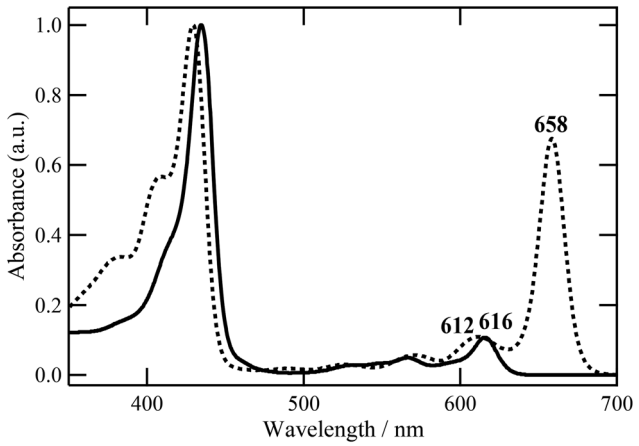

Fig. 7 Electronic absorption spectra of **ZnC** (dotted line) and **ZnP** (solid line) in 1% (v/v) methanol and benzene. Both the spectra are normalized at the intense Soret maxima.

enhanced CD bands in a red-shifted Qy band region (Fig. 6, lower part).

In 1% (v/v) methanol and benzene, Qy bands of **ZnC–ZnP** were observed at 671 and 627 nm, which were shifted to longer wavelengths than the Qy(0,0) maximum of the **ZnC** monomer at 658 nm and that of **ZnP** at 616 nm, respectively (Fig. 7). The former 671 nm band would be produced by the excitonic coupling of the main Qy(0,0) band of the zinc chlorin moiety with the Qy(0,0) band of the zinc porphyrin moiety in the J-type conformer. The latter 627 nm band is ascribable to the interaction of the minor Qy(0,1) vibrational band of the zinc chlorin moiety at 612 nm with the Qy(0,0) band of the zinc porphyrin moiety. The red-shifted values and the band intensities are dependent on the energy levels and intensities of the interacting bands. The difference between the energy levels decreases, and the component bands showed an increase in intensity, exhibiting a larger red-shift and a larger band through excitonic coupling. This explanation is supported by the excitonic coupling theory.[26] The 671 nm band was shifted to a longer wavelength by 290 cm^{-1} than the Qy(0,0) maximum of **ZnC** at 658 nm, while the 627 nm band was red-shifted by 280 cm^{-1} compared to that of **ZnP** at 616 nm. The similar red-shifted values are explained by the following two compensative

factors. The energy difference between the Qy(0,0) states of **ZnC** and **ZnP** (1040 cm^{-1}) was 10-fold larger than that between the Qy(0,1) of **ZnC** and Qy(0,0) of **ZnP** (110 cm^{-1}), and the Qy (0,0) band of **ZnC** was 6-fold more intense than its Qy(0,1) band. These factors also led to the observation that the 671 nm band was about 2.5-fold larger than the 627 nm band.

Similarly as in the above **ZnC–ZnP** heterodyad, the electronic absorption and CD spectra showed that the zinc bacteriochlorin and zinc chlorin moieties in **ZnB–ZnC** hardly interacted intramolecularly in 1% (v/v) pyridine–benzene, but π–π stacked in 1% (v/v) methanol–benzene to form a folded conformer by the linkage of two methanol molecules using the coordination of Zn···O (methanol) and hydrogen bond of 13-C═O···H–O (methanol) (Fig. 8). In the 1% (v/v) methanol–benzene solution of **ZnB–ZnC**, two intense peaks in the Qy region appeared at 787 and 673 nm and one more small band between the two bands was observed at around 715 nm, which was estimated from the second derivative spectrum (see Fig. S3†). These three bands were also confirmed by Gaussian deconvolutional analysis.

The above three bands could be produced from the following excitonically interacting bands, as explained for **ZnC–ZnP** (*vide supra*). In 1% (v/v) methanol–benzene, the **ZnB** monomer gave the main Qy(0,0) band at 773 nm with a small shoulder at around 701 nm as the Qy(0,1) maximum and a less intense shoulder at approximately 639 nm as the Qy(0,2) second vibrational band (the solid line in Fig. 9). The latter two peak wavelengths were estimated from the second derivative spectrum (Fig. S4†), and the energy difference between the Qy(0,0) and Qy(0,1) states (1330 cm^{-1}) was almost identical to that between the Qy(0,1) and Qy(0,2) states (1380 cm^{-1}). The 787- and 715 nm bands are attributed to the excitonic coupling of

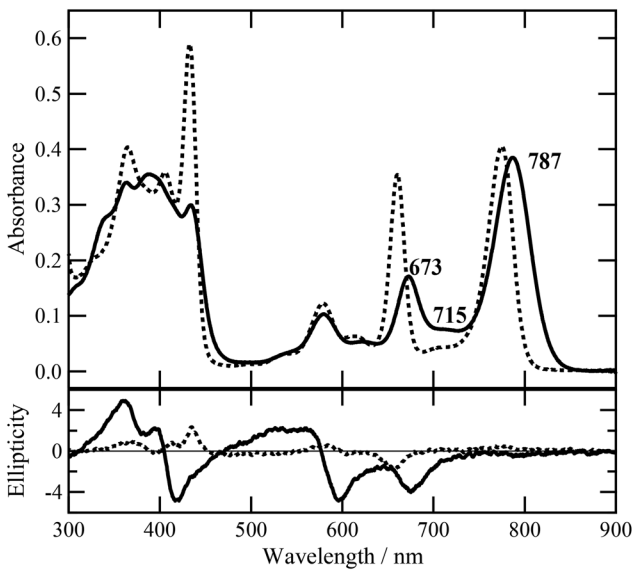

Fig. 8 Electronic absorption (upper) and CD spectra (lower) of **ZnB–ZnC** (5 μM) in benzene with 1% (v/v) methanol (solid lines) and pyridine (dotted lines).

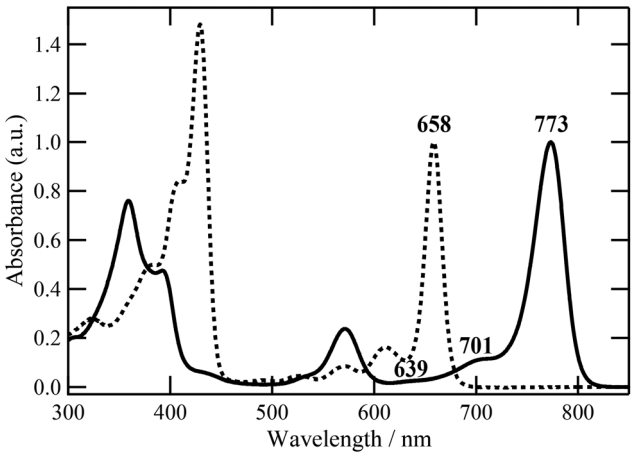

Fig. 9 Electronic absorption spectra of **ZnB** (solid line) and **ZnC** (dotted line) in 1% (v/v) methanol and benzene. Both the spectra are normalized at the Qy(0,0) maxima.

the Qy(0,0) and Qy(0,1) bands of the zinc bacteriochlorin moiety (773 and 701 nm), respectively, with the Qy(0,0) band of the zinc chlorin moiety (658 nm) in the folded **ZnB–ZnC** conformer assisted by methanol. The two peaks were bathochromically shifted by 230 and *ca.* 280 cm^{-1} from the Qy(0,0) and Qy(0,1) states, respectively, of the zinc bacteriochlorin monomer. The comparable red-shifted values are ascribable to the approximately 10-fold intensity of the Qy(0,0) band over the Qy(0,1) band of zinc bacteriochlorin and the large energy difference between the former and the Qy(0,0) band of zinc chlorin in comparison with that between the latter and the Qy (0,0) band of zinc chlorin (2260 > 930 cm^{-1}). The 673 nm band was based on the excitonic coupling of the relatively intense Qy(0,0) band of the zinc chlorin moiety (658 nm) with the faint Qy(0,2) band of zinc bacteriochlorin (≈639 nm) in the methanol-locked **ZnB–ZnC** conformer.

Conclusion

Here, we experimentally demonstrated that a Chl-*a* derivative possessing a chlorin π-skeleton excitonically interacted with another Chl-*a* derivative bearing a porphyrin π-system and a BChl-*a* derivative bearing a bacteriochlorin π-system to give red-shifted Qy absorption bands. The bathochromic shifts are ascribable to the exciton coupling of the two different π-conjugated systems in synthetic heterodyads. The red-shifted bands in their folded conformers were constructed by the J-type interaction of the main Qy band of a higher site-energy component with the main Qy and its minor vibrational bands of a lower site-energy component (see Fig. S5†). This observation would be useful for the determination of site energies of Chl-*a*/*c* dimers in FCPs and also for the investigation of electron-transferring processes from BChls-*a*/*g* or their 13^2-epimeric BChls-*a*′/*g*′ to Chl-*a* species in PS1-type RCs of anoxygenic photosynthetic bacteria.

Conflicts of interest

There are no conflicts of interest to declare.

Acknowledgements

We thank Dr Chihiro Azai of Ritsumeikan University and Dr Yuichi Kitagawa of Hokkaido University for providing useful information and Dr Shin Ogasawara of Ritsumeikan University for preparation of drawings. This work was partially supported by the JSPS KAKENHI Grant Number JP17H06436 in Scientific Research on Innovative Areas "Innovation for Light-Energy Conversion (I^4LEC)".

References

1 H. Tamiaki, R. Shibata and T. Mizoguchi, The 17-propionate function of (bacterio)chlorophylls: biological implication of their long esterifying chains in photosynthetic systems, *Photochem. Photobiol.*, 2007, **83**, 152–162.
2 Y. Umena, K. Kawakami, J. R. Shen and N. Kamiya, Crystal structure of oxygen-evolving photosystem II at a resolution of 1.9 Å, *Nature*, 2011, **473**, 55–60.
3 G. Feher, J. P. Allen, M. Y. Okamura and D. C. Rees, Structure and function of bacterial photosynthetic reaction centres, *Nature*, 1989, **339**, 111–116.
4 B. R. Green, After the primary endosymbiosis: an update on the chromalveolate hypothesis and the origins of algae with Chl *c*, *Photosynth. Res.*, 2011, **107**, 103–115.
5 W. Wang, L.-J. Yu, C. Xu, T. Tomizaki, S. Zhao, Y. Umena, X. Chen, X. Qin, Y. Xin, M. Suga, G. Han, T. Kuang and J.-R. Shen, Structural basis for blue-green light harvesting and energy dissipation in diatoms, *Science*, 2019, **363**, aav0365.
6 J. C. Zill, Z. He, M. Tank, B. H. Ferlez, D. P. Canniffe, Y. Lahav, P. Bellstedt, A. Alia, I. Schapiro, J. H. Golbeck, D. A. Bryant and J. Matysik, ^{15}N photo-CIDNP MAS NMR analysis of reaction centers of *Chloracidobacterium thermophilum*, *Photosynth. Res.*, 2018, **137**, 295–305.
7 C. Gisriel, I. Sarrou, B. Ferlez, J. H. Golbeck, K. E. Redding and R. Fromme, Structure of a symmetric photosynthetic reaction center-photosystem, *Science*, 2017, **357**, 1021–1025.
8 C. Azai, K. Kim, T. Kondo, J. Harada, S. Itoh and H. Ohoka, A heterogeneous tag-attachment to the homodimeric type 1 photosynthetic reaction center core protein in the green sulfur bacterium *Chlorobaculum tepidum*, *Biochim. Biophys. Acta, Bioenerg.*, 2011, **1807**, 803–812.
9 G. S. Orf and R. E. Blankenship, Chlorosome antenna complexes from green photosynthetic bacteria, *Photosynth. Res.*, 2013, **116**, 315–331.
10 J. Harada, Y. Shibata, M. Teramura, T. Mizoguchi, Y. Kinoshita, K. Yamamoto and H. Tamiaki, In vivo energy transfer from bacteriochlorophyll *c*, *d*, *e*, or *f* to bacteriochlorophyll *a* in wild-type and mutant cells of the green sulfur bacterium *Chlorobaculum limnaeum*, *ChemPhotoChem*, 2018, **2**, 190–195.
11 V. L. Gunderson and M. R. Wasielewski, Supramolecular chlorophyll assemblies for artificial photosynthesis, *Handb. Porphyrin Sci.*, 2012, **20**, 45–105, DOI: 10.1142/9789814335508_0022.
12 H. Tamiaki, T. Tatebe and Y. Kitagawa, Covalently linked dimer of chlorophyll-*a* derivative with an amide bond and its folded conformer, *Tetrahedron Lett.*, 2018, **59**, 3120–3123.
13 S. G. Boxer and G. L. Closs, A covalently bound dimeric derivative of pyrochlorophyllide *a*. A possible model for reaction center chlorophyll, *J. Am. Chem. Soc.*, 1976, **98**, 5406–5408.
14 M. R. Wasielewski, M. H. Studier and J. J. Katz, Covalently linked chlorophyll *a* dimer: A biomimetic model of special pair chlorophyll, *Proc. Natl. Acad. Sci. U. S. A.*, 1976, **73**, 4282–4286.
15 H. Tamiaki, K. Fukai, H. Shimazu, K. Nishide, Y. Shibata, S. Itoh and M. Kunieda, Covalently linked zinc chlorophyll dimers as a model of a chlorophyllous pair in photosynthetic reaction centers, *Photochem. Photobiol. Sci.*, 2008, **7**, 1231–1237.
16 H. Tamiaki, K. Fukai, H. Shimazu and S. Shoji, Synthesis of zinc chlorophyll homo/hetero-dyads and their folded conformers with porphyrin, chlorin and bacteriochlorin π-systems, *Photochem. Photobiol.*, 2014, **90**, 121–128.
17 M. R. Wasielewski and W. A. Svec, Synthesis of covalently linked dimeric derivatives of chlorophyll *a*, pyrochlorophyll *a*, chlorophyll *b*, and bacteriochlorophyll *a*, *J. Org. Chem.*, 1980, **45**, 1969–1974.
18 S. Shoji, Y. Nomura and H. Tamiaki, Heterodimers of zinc and free-base chlorophyll derivatives co-assembled in biomimetic chlorosomal J-aggregates, *Photochem. Photobiol. Sci.*, 2019, **18**, 555–562.
19 H. Tamiaki, T. Watanabe and T. Miyatake, Facile synthesis of 13^1-oxo-porphyrins possessing reactive 3-vinyl or 3-formyl group, protochlorophyll-*a*/*d* derivatives by 17,18-dehydrogenation of chlorins, *J. Porphyrins Phthalocyanines*, 1999, **3**, 45–52.
20 H. Tamiaki, S. Yagai and T. Miyatake, Synthetic zinc tetrapyrroles complexing with pyridine as a single axial ligand, *Bioorg. Med. Chem.*, 1998, **6**, 2171–2178.
21 R. J. Abraham, K. M. Smith, D. A. Goff and J.-J. Lai, NMR spectra of porphyrins. 18. A ring-current model for chlorophyll derivatives, *J. Am. Chem. Soc.*, 1982, **104**, 4332–4337.
22 Y. Saga, S. Hojo and Y. Hirai, Comparison of demetalation properties between zinc chlorin and zinc porphyrin derivatives: effect of macrocyclic structures, *Bioorg. Med. Chem.*, 2010, **18**, 5697–5700.
23 H. Tamiaki, S. Takeuchi, S. Tsudzuki, T. Miyatake and R. Tanikaga, Self-aggregation of synthetic zinc chlorins with a chiral 1-hydroxyethyl group as a model for *in vivo* epimeric bacteriochlorophyll-*c* and *d* aggregates, *Tetrahedron*, 1998, **54**, 6699–6718.

24 H. Tamiaki, M. Kouraba, K. Takeda, S. Kondo and R. Tanikaga, Asymmetric synthesis of methyl bacteriopheophorbide-*d* and analogues by stereoselective reduction of the 3-acetyl to the 3-(1-hydroxyethyl) group, *Tetrahedron: Asymmetry*, 1998, **9**, 2101–2111.
25 H. Tamiaki, T. Miyatake, R. Tanikaga, A. R. Holzwarth and K. Schaffner, Self-assembly of an artificial light-harvesting antenna: energy transfer from a zinc chlorin to a bacteriochlorin in a supramolecular aggregate, *Angew. Chem., Int. Ed. Engl.*, 1996, **35**, 772–774.
26 Y. Kitagawa, J. Hiromoto and K. Ishii, Electronic absorption, MCD, and luminescence properties of porphyrin J-aggregates, *J. Porphyrins Phthalocyanines*, 2013, **17**, 703–711.